

# Design and Synthesis of New Circularly Polarized Thermally Activated Delayed Fluorescence Emitters

Sophie Feuillastre,<sup>†, ∇</sup> Mathilde Pauton,<sup>†, ∇</sup> Longhui Gao,<sup>†</sup> Alaric Desmarchelier,<sup>†</sup> Adrian J. Riives,<sup>‡</sup> Damien Prim,<sup>§</sup> Denis Tondelier,<sup>||</sup> Bernard Geffroy,<sup>||, ⊥</sup> Gilles Muller,<sup>‡</sup> Gilles Clavier,<sup>#</sup> and Grégory Pieters<sup>\*, †</sup>

<sup>†</sup>SCBM, CEA, Université Paris Saclay, F-91191, Gif-sur-Yvette, France

<sup>‡</sup>Department of Chemistry, San José State University, One Washington Square, San José, California 95192-0101, United States

<sup>§</sup>Université de Versailles-St-Quentin-en-Yvelines, ILV, UMR CNRS 8180, 45 Avenue des États-Unis, 78035 Versailles Cedex, France

<sup>||</sup>LPICM, CNRS, Ecole Polytechnique, Université Paris Saclay, 91128, Palaiseau, France

<sup>⊥</sup>LICSEN, NIMBE, CEA, CNRS, Université Paris Saclay, CEA 91191 Gif-sur-Yvette Cedex, France

<sup>#</sup>PPSM, ENS Cachan, CNRS, Université Paris-Saclay, 94235 Cachan, France

## Supporting Information

**ABSTRACT:** This work describes the first thermally activated delayed fluorescence material enabling circularly polarized light emission through chiral perturbation. These new molecular architectures obtained through a scalable one-pot sequential synthetic procedure at room temperature (83% yield) display high quantum yield (up to 74%) and circularly polarized luminescence with an absolute luminescence dissymmetry factor,  $|g_{lum}|$ , of  $1.3 \times 10^{-3}$ . These chiral molecules have been used as an emissive dopant in an organic light emitting diode exhibiting external quantum efficiency as high as 9.1%.

The discovery of efficient thermally activated delayed fluorescence (TADF) materials and small organic molecules enabling circularly polarized luminescence emission (CPL-SOMs) is crucial for the development of future optical and photonic devices.<sup>1,2</sup> In TADF emitters both singlet and triplet excitons can be harvested for light emission by a reverse intersystem crossing process thanks to a small energy gap between their singlet and triplet states ( $\Delta E_{ST}$ ). This property has recently motivated numerous research works because of the theoretical possibility to develop organic light emitting diodes (OLEDs) with maximum efficiency.<sup>3</sup> The conception of CPL-SOMs is also a great challenge for organic chemists. Currently, only a small number of CPL-SOMs display high performance both in terms of quantum yield ( $\phi_F$ ) and luminescence dissymmetry factor ( $g_{lum}$ ).<sup>4</sup> Moreover, such enantiopure compounds are usually obtained after numerous synthetic steps or require enantiomeric separation through preparative HPLC, restricting their potential application because of lack of cost-effectiveness.<sup>5</sup> As a consequence, rapid, easy, and flexible access to more performant CPL-SOMs is required in order to unlock their tremendous technological potential.<sup>6</sup> In the context of OLED devices, CPL emitters are appealing in order to decrease the energy loss arising from the required use of a polarizer and a quarter-wave plate for the attenuation of the external light reflection (50% of the light emitted is absorbed by

the polarizer for standard molecules).<sup>7</sup> For CPL-SOMs, TADF properties can be advantageous for their overall photophysical properties (high quantum yield, long fluorescence lifetime). In other words, the design of new molecular architectures presenting both TADF and CPL emission properties can be considered as a cornerstone for enhancement of the performances of different types of devices (optical displays, optical storage and processing systems, spintronics-based devices). Hirata et al. have recently described a molecule exhibiting both TADF and CPL emission.<sup>8</sup> Their elegant design relies on the introduction of a chiral carbon center sandwiched between a donor and an acceptor moiety. Their approach consists in the synthesis of a racemic mixture followed by separation of both enantiomers using chiral preparative HPLC. However, although typical  $|g_{lum}|$  values were measured ( $1.1 \times 10^{-3}$ ), this molecule has a very moderate fluorescence quantum yield ( $\phi_F = 4\%$  in toluene), and its use as an emissive dopant in an OLED has not been reported. Here, we describe the design of a new TADF material enabling CPL through chiral perturbation by a tethered chiral unit (Figure 1). Obtained via a one-pot sequential

### TADF emitter



### Chiral perturbing unit

- CPL & TADF
- One-pot synthesis (83% yield)
- High quantum yield (up to 74%)
- High racemization barrier

Figure 1. Molecular design of 1.

Received: January 24, 2016

Published: March 11, 2016

synthesis, molecular architectures **1** are highly luminescent ( $\phi_F = 53\%$  in degassed toluene), possess  $|g_{\text{lum}}|$  values of  $1.3 \times 10^{-3}$ , and can be used as emissive dopants in OLEDs displaying high external quantum efficiency.

Very recently, de la Moya et al. have brought to light a new concept for the development of CPL-SOMs. In their approach, tethering an orthogonal chiral unit to an acting achiral chromophore enabled CPL activity. To date, only two types of structures, both based on metal (Zn) or metalloid (B) dipyrin complexes exploiting this concept have been reported.<sup>9</sup> We envisioned that such a chiral perturbation could also enable CPL on a chromophore in a purely organic molecular structure, through an appropriate design, allowing the control over the localization of the frontier orbitals. One example illustrating this concept is molecule **1** which can exhibit both TADF and CPL properties. As depicted in Figure 2, the geometry optimization of

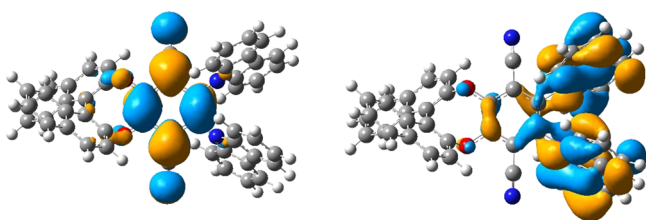
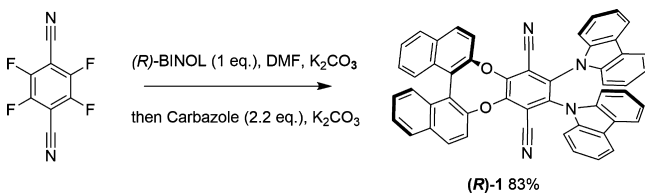


**Figure 2.**  $S_0$  state optimization by DFT calculation of (*R*)-**1**: HOMO is depicted on the right and LUMO on the left.

**1** (see SI for details) shows that the HOMO is mainly localized on the carbazole units and the LUMO on the dicyanobenzene moiety.<sup>10</sup> Such a spatial separation of HOMO/LUMO is now well established as a key feature in order to obtain a small  $\Delta E_{\text{ST}}$  required for TADF. This localization also implies the non-participation of the 1,1'-binaphthyl moiety in the acting chromophore, but the close proximity of this chiral unit may efficiently perturb the TADF emitter in order to enable electronic circular dichroism (ECD) and CPL activities.

The enantiopure target molecules, (*R*)-**1** and (*S*)-**1**, were obtained through an optimized cost-effective one-pot sequential procedure involving commercially available compounds (Scheme 1). A highly selective dissymmetrization of the starting

#### Scheme 1. One-Pot Sequential Synthesis of (*R*)-**1**



tetrafluoroterephthalonitrile, involving enantiopure BINOL and  $K_2CO_3$  as a base, has allowed the formation of the chiral difluorinated intermediate **2** (which can be isolated in 88% yield, see SI). Then, carbazole (2.2 equiv) and additional  $K_2CO_3$  were added to the reaction mixture, leading to the target molecule with an overall yield of 83% after purification over silica gel. This easy and straightforward procedure has permitted the synthesis of both enantiomers of **1** with high enantiomeric excess (>99%, based on chiral HPLC, see SI) starting from enantiopure BINOL on a half-gram scale.

Steady-state photophysical studies have first been conducted on (*R*)-**1** in various solvents. Absorption spectra display a visible

band centered around 420 nm which is not very intense ( $\epsilon_{419}(\text{DCM}) = 3000 \text{ mol}\cdot\text{L}^{-1}\cdot\text{cm}^{-1}$ ) because of the spatial decorrelation of the orbitals involved in the transition. There are also more intense bands in the UV region centered at 330 and 290 nm. It must be pointed out that the absorption spectra of (*R*)-**1** are not solvent-dependent. On the other hand, the fluorescence spectra and fluorescence quantum yields are strongly solvent dependent, which was already reported for compounds with related structures.<sup>11</sup>

The maximum emission wavelength goes from 486 nm in cyclohexane to 573 nm in ethanol (color of emission goes from cyan to orange; Figure 3), and fluorescence quantum yields

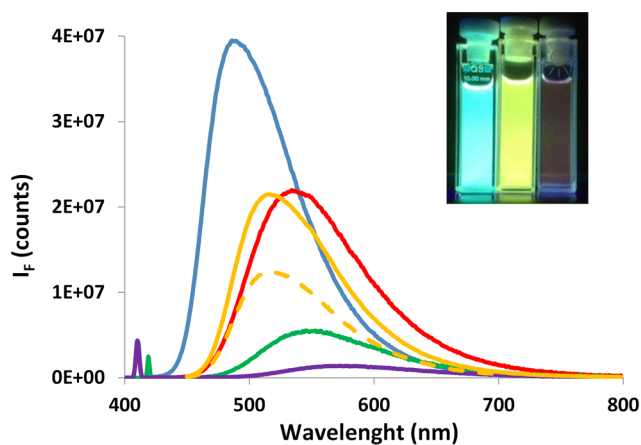


**Figure 3.** Fluorescence spectra ( $C = 10^{-5} \text{ M}$ ) of (*R*)-**1** in cyclohexane (blue), THF (red), nondegassed toluene (orange dashed line) and argon degassed (orange solid line), dichloromethane (green), and ethanol (purple);  $\lambda_{\text{ex}} = 410 \text{ nm}$ . Inset picture: fluorescence under 365 nm excitation of (*R*)-**1** in cyclohexane, THF, and ethanol (from left to right).

decrease from 0.74 to 0.06 in the same solvents. The solvent effect on the fluorescence bands was studied following the methodology developed by Catalán,<sup>12</sup> in which the various types of solute–solvent interactions are described thanks to four independent solvent parameters (see SI for details). It was found that the band position is mainly influenced by solvent polarizability. Fluorescence emission of (*R*)-**1** in toluene was recorded both in aerated and argon-degassed solutions. The fluorescence quantum yield is increased from 0.28 to 0.53 in the absence of triplet-quenching oxygen, and the normalized spectra are identical. Thus, (*R*)-**1** is TADF active and  $\Phi_{\text{TADF}} = 0.25$ . Fluorescence decays of (*R*)-**1** were recorded in toluene (Figure 4) at two different time scales (90 ns and 10  $\mu\text{s}$ ). In the rapid regime a monoexponential decay was recorded with a fluorescence lifetime of 16 ns (both in the presence and absence of oxygen, see SI). In the long time regime, a complex decay is obtained before degassing and a biexponential one after argon purging. The fitting gave a short lifetime of 20 ns and a long one of 2.9  $\mu\text{s}$  which confirms that (*R*)-**1** emits both prompt and delayed fluorescence. From these data the rates of the various processes were calculated. The intersystem crossing rate ( $k_{\text{isc}} = 9.4 \times 10^6 \text{ s}^{-1}$ ) is faster than the singlet-state radiative rate ( $k_r(S) = 5.0 \times 10^6 \text{ s}^{-1}$ ) allowing the singlet to triplet crossing.

The reversed ISC rate is much slower ( $k_{\text{risc}} = 1.9 \times 10^5 \text{ s}^{-1}$ ), and delayed fluorescence rate is  $k_D = 8.7 \times 10^4 \text{ s}^{-1}$ . These values mean that after excitation, molecule (*R*)-**1** can emit light and populate T1 at about the same rate and subsequent TADF is

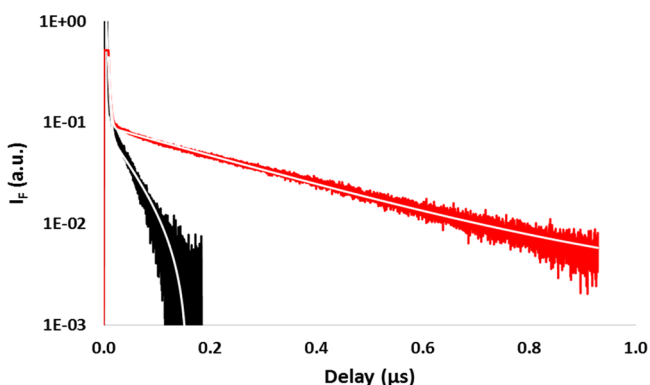


**Figure 4.** Fluorescence decays of (*R*)-1 in aerated (black) and argon-purged toluene solutions (red); the solid (white) lines are the biexponential fits ( $\lambda_{\text{ex}} = 400 \text{ nm}$ ).

possible. These findings corroborate that the architectural approach considered leads to TADF active molecules. Fluorescence decays were also recorded at different wavelengths. The reconstructed spectra at different delays match the steady-state one (see SI).

To further characterize the system of interest, the chiroptical properties of **1** in the ground and excited states were investigated by ECD and CPL spectroscopy, respectively. The toluene solution ECD spectra of each enantiomeric form of **1**, (*R*)-1 and (*S*)-1, are shown in Figure 5a. This enantiomeric relationship was confirmed by the observation of mirror-image ECD spectra for (*R*)-1 and (*S*)-1.

In the visible region of the ECD spectrum of each enantiomeric form of **1** a signal is observed for the band centered around 420 nm. This is a key feature of the ECD spectra to highlight since it is indicative that the designed chiral perturbation is affecting the TADF emitter, at least in its ground state. On the other hand, we have selected CPL, the emission

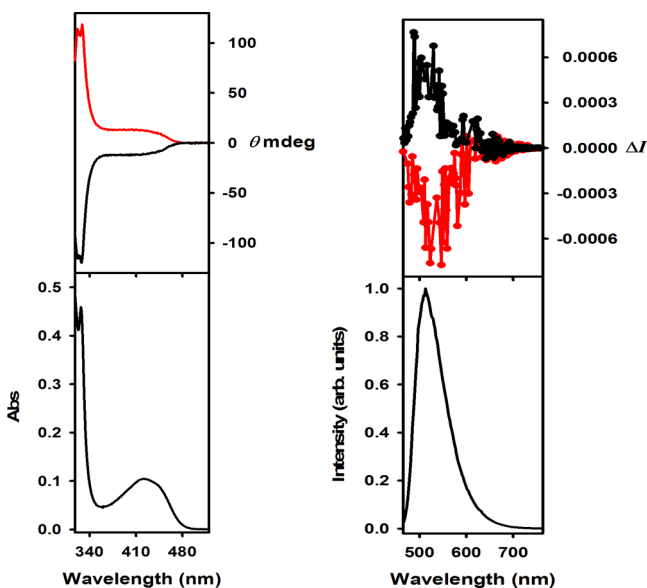


**Figure 5.** (a) ECD spectra ( $1.5 \times 10^{-3} \text{ M}$ , upper curves) of (*R*)-1 (red curve) and (*S*)-1 (black curve) in toluene and UV spectrum (ca.  $10^{-5} \text{ M}$ , lower curve) at 295 K. (b) CPL (upper curves) and total luminescence (lower curves) spectra of (*R*)-1 (red curve) and (*S*)-1 (black curve) in degassed toluene (ca.  $10^{-3} \text{ M}$ ) at 295 K, upon excitation at 460 and 450 nm, respectively.

analog to ECD, to further investigate the chiroptical properties of **1**. The CPL and total luminescence spectra measured for each enantiomeric form of **1**, (*R*)-1 and (*S*)-1, in degassed toluene solutions at 295 K are shown in Figure 5b. Satisfactorily, CPL was detected from (*R*)-1 and (*S*)-1, but also almost mirror CPL spectra were recorded. This CPL behavior confirms that this new TADF material enables CPL through the chiral perturbation of a tethered chiral unit as well as an ECD activity as mentioned earlier. Although the  $|g_{\text{lum}}|$  values are relatively small and in the order of  $1.3 \times 10^{-3}$  (a typical value for CPL-SOMs), as determined at the maximum emission wavelength, one can see that the CPL activity observed for the two enantiomeric forms of **1** corroborates the objective of this work. That is, the preparation of a TADF material enabling ECD and CPL properties, and that the proposed molecular architecture approach is doable, and more importantly promising to develop TADF materials showing measurable and distinctive CPL. The emitted light was polarized in opposite directions for the two enantiomeric forms of **1**. This can be explained by the fact that the polarizability direction of the CPL signal was induced by the chiral perturbation of the tethered chiral unit.

Molecule (*S*)-1 has then been used as an emissive dopant in an OLED with the following structure: glass/ITO/CuPc/ $\alpha$ -NBP/TcTa/mCP:(*S*)-1/TmPyPB/LiF/Al (see SI for more details). As shown in Figure 6, the electroluminescence (EL) spectrum of

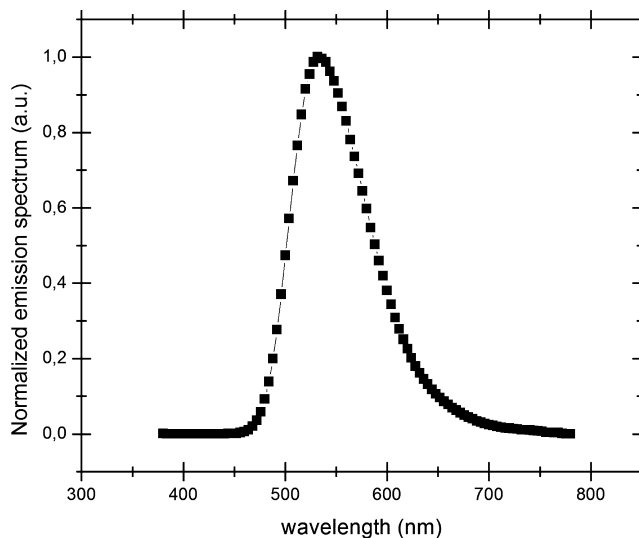


**Figure 6.** Normalized emission spectrum of the OLED with 20 wt % of (*S*)-1 in mCP recorded at  $10 \text{ mA}\cdot\text{cm}^{-2}$ .

the OLED shows only the emission of the guest material (*S*)-1 suggesting a complete energy transfer from the host (mCP) to the guest. The EL spectrum is in good agreement with the photoluminescent spectrum of the material (*R*)-1 reported in toluene in Figure 3. The best performance of these OLED devices has been recorded with 20 wt % of (*S*)-1 in mCP (see SI). The device emits light at 4 V, with a maximum current efficiency (CE) of  $34.7 \text{ cd}\cdot\text{A}^{-1}$ , a maximum power efficiency (PE) of  $16.3 \text{ lm}\cdot\text{W}^{-1}$ , and an external quantum efficiency (EQE) of 9.1%. These high values achieved in our devices confirm that the EL emission is coming from triplet states harvested from TADF.

Performance shows that the electronic transfer from the host to the guest material is very efficient and leads to notable optoelectrical efficiencies. Moreover, no racemization has been detected during the fabrication process of the OLED device (see

SI for details). Both high EQE and configurational stability demonstrate that this new molecular design is viable for the future development of efficient polarized OLED devices.

In summary, this communication describes the development of the first purely organic molecule where CPL is enabled on a single acting achiral chromophore through chiral perturbation. The advantage of this approach is illustrated by the easy (one-pot synthesis) and efficient (83% yield) access to molecules exhibiting both TADF and CPL properties starting from commercially available compounds. These new chiral molecular architectures possess high standard photophysical properties such as high quantum efficiency (up to 74%), long fluorescence lifetime ( $\mu\text{s}$  range), and  $|g_{\text{lum}}|$  values of  $1.3 \times 10^{-3}$ . Moreover, they can be incorporated without racemization in OLED devices as emissive dopants offering a high EQE (9.1%). We believe that the molecular design described here paves the way not only to the development of new CPL-SOMs presenting high photo- and electroluminescence performances but also to innovative chiroptical switches and sensors with an easy, scalable, time- and cost-effective synthetic route.

## ■ ASSOCIATED CONTENT

### Supporting Information

The Supporting Information is available free of charge on the ACS Publications website at DOI: 10.1021/jacs.6b00850.

Experimental details and data (PDF)

## ■ AUTHOR INFORMATION

### Corresponding Author

\*gregory.pieters@cea.fr

### Author Contributions

<sup>v</sup>These authors contributed equally.

### Notes

The authors declare no competing financial interest.

## ■ ACKNOWLEDGMENTS

G.P. thanks LabEx Charm3at (ANR-11-LABEX-0039) and CEA for financial support, Dr. Bernard Rousseau, Céline Chollet, and David Buisson for Chiral HPLC analysis, Pr. Fabien Miomandre for his help with electrochemistry. G.M. thanks the NIH, Minority Biomedical Research Support (grant 1 SC3 GM089589-06), and the Henry Dreyfus Teacher-Scholar Award for financial support, whereas A.J.R. thanks the SJSU RISE program (NIH grant 5R25GM71381) for a research fellowship.

## ■ REFERENCES

- (1) Tao, Y.; Yuan, K.; Chen, T.; Xu, P.; Li, H.; Chen, R.; Zheng, C.; Zhang, L.; Huang, W. *Adv. Mater.* **2014**, *26*, 7931.
- (2) Sánchez-Carnerero, E. M.; Agarrabeitia, A. R.; Moreno, F.; Maroto, B. L.; Muller, G.; Ortiz, M. J.; de la Moya, S. *Chem. - Eur. J.* **2015**, *21*, 13488.
- (3) For recent examples see: (a) Kaji, H.; Suzuki, H.; Fukushima, T.; Shizu, K.; Suzuki, K.; Kubo, S.; Komino, T.; Oiwa, H.; Suzuki, F.; Wakamiya, A.; Murata, Y.; Adachi, C. *Nat. Commun.* **2015**, *6*, 8476. (b) Kawasumi, K.; Wu, T.; Zhu, T.; Chae, H. S.; Van Voorhis, T.; Baldo, M. A.; Swager, T. M. *J. Am. Chem. Soc.* **2015**, *137*, 11908. (c) Zhang, Q.; Kuwabara, H.; Potscavage, W. J., Jr.; Huang, S.; Hatae, Y.; Shibata, T.; Adachi, C. *J. Am. Chem. Soc.* **2014**, *136*, 18070. (d) Hirata, S.; Sakai, Y.; Masui, K.; Tanaka, H.; Lee, S. Y.; Nomura, H.; Nakamura, N.; Yasumatsu, M.; Nakanotani, H.; Zhang, Q.; Shizu, K.; Miyazaki, H.; Adachi, C. *Nat. Mater.* **2015**, *14*, 330. (e) Tsai, W.-L.; Huang, M.-H.; Lee, W.-K.; Hsu, Y.-J.; Pan, K.-C.; Huang, Y.-H.; Ting, H.-C.; Sarma, M.;

Ho, Y.-Y.; Hu, H.-C.; Chen, C.-C.; Lee, M. T.; Wong, K.-T.; Wu, C.-C. *Chem. Commun.* **2015**, *51*, 13662. (f) Liu, M.; Seino, Y.; Chen, D.; Inomata, S.; Su, S.-J.; Sasabe, H.; Kido, J. *Chem. Commun.* **2015**, *51*, 16353. (g) Lee, D. R.; Kim, M.; Jeon, S. K.; Hwang, S.-H.; Lee, C. W.; Lee, J. Y. *Adv. Mater.* **2015**, *27*, 5861. (h) Suzuki, K.; Kubo, S.; Shizu, K.; Fukushima, T.; Wakamiya, A.; Murata, Y.; Adachi, C.; Kaji, H. *Angew. Chem., Int. Ed.* **2015**, *54*, 15231.

(4) The degree of CPL is given by the luminescence dissymmetry factor,  $g_{\text{lum}}(\lambda) = 2\Delta I/I = 2(IL - IR)/(IL + IR)$ , where IL and IR refer, respectively, to the intensity of left and right circularly polarized emissions.

(5) (a) Sawada, Y.; Furumi, S.; Takai, A.; Takeuchi, M.; Noguchi, K.; Tanaka, K. *J. Am. Chem. Soc.* **2012**, *134*, 4080. (b) Nakamura, K.; Furumi, S.; Takeuchi, M.; Shibuya, T.; Tanaka, K. *J. Am. Chem. Soc.* **2014**, *136*, 5555. (c) Morisaki, Y.; Gon, M.; Sasamori, T.; Tokitoh, N.; Chujo, Y. *J. Am. Chem. Soc.* **2014**, *136*, 3350. (d) Gon, M.; Morisaki, Y.; Chujo, Y. *J. Mater. Chem. C* **2015**, *3*, 521.

(6) (a) Schadt, M. *Annu. Rev. Mater. Sci.* **1997**, *27*, 305. (b) Wagenknecht, C.; Li, C.-M.; Reingruber, A.; Bao, X.-H.; Goebel, A.; Chen, Y.-A.; Zhang, Q.; Chen, K.; Pan, J.-W. *Nat. Photonics* **2010**, *4*, 549. (c) Sherson, J. F.; Krauter, H.; Olsson, R. K.; Julsgaard, B.; Hammerer, K.; Cirac, I.; Polzik, E. S. *Nature* **2006**, *443*, 557. (d) Farshchi, R.; Ramsteiner, M.; Herfort, J.; Tahraoui, A.; Grahn, H. T. *Appl. Phys. Lett.* **2011**, *98*, 162508. (e) Jan, C. M. *Opt. Express* **2011**, *19*, 5431. (f) Yu, C. J.; Lin, C. E.; Yu, L. P.; Chou, C. *Appl. Opt.* **2009**, *48*, 758.

(7) Kim, B. C.; Lim, Y. J.; Song, J. H.; Lee, J. H.; Jeong, K.-U.; Lee, J. H.; Lee, G.-D.; Lee, S. H. *Opt. Express* **2014**, *22*, 1725.

(8) Imagawa, T.; Hirata, S.; Totani, K.; Watanabe, T.; Vacha, M. *Chem. Commun.* **2015**, *51*, 13268.

(9) (a) Sanchez-Carnerero, E. M.; Moreno, F.; Maroto, B. L.; Agarrabeitia, A. R.; Ortiz, M. J.; Vo, B. G.; Muller, G.; de La Moya, S. *J. Am. Chem. Soc.* **2014**, *136*, 3346. (b) Kögel, J. F.; Kusaka, S.; Sakamoto, R.; Iwashima, T.; Tsuchiya, M.; Toyoda, R.; Matsuoka, R.; Tsukamoto, T.; Yuasa, J.; Kitagawa, Y.; Kawai, T.; Nishihara, H. *Angew. Chem., Int. Ed.* **2016**, *55*, 1377. (c) Zhang, S.; Wang, Y.; Meng, F.; Dai, C.; Cheng, Y.; Zhu, C. *Chem. Commun.* **2015**, *51*, 9014.

(10) (a) Uoyama, H.; Goushi, K.; Shizu, K.; Nomura, H.; Adachi, C. *Nature* **2012**, *492*, 234. (b) Ishimatsu, R.; Matsunami, S.; Kasahara, T.; Mizuno, J.; Edura, T.; Adachi, C.; Nakano, K.; Imato, T. *Angew. Chem., Int. Ed.* **2014**, *53*, 6993.

(11) Ishimatsu, R.; Matsunami, S.; Shizu, K.; Adachi, C.; Nakano, K.; Imato, T. *J. Phys. Chem. A* **2013**, *117*, 5607.

(12) Catalàn, J. *J. Phys. Chem. B* **2009**, *113*, 5951.